Oligomerisation of Ethylene by Bis(imino)pyridyliron and -cobalt Complexes

George J.P. Britovsek,[a] Sergio Mastroianni,[a] Gregory A. Solan,[a] Simon P. D. Baugh,[a] Carl Redshaw,[a] Vernon C. Gibson,*[a] Andrew J. P. White,[a] David J. Williams,[a] and Mark R. J. Elsegood[b]

Dedicated to Professor Wilhelm Keim on the occasion of his 65th birthday

Abstract: A series of bis(imino)pyridyliron and -cobalt complexes [{2,6-(CR=NAr)$_2$C$_5$H$_3$N}MX$_2$] (R = H, Me; M = Fe, Co; X = Cl, Br) **8**–**16** containing imino-aryl rings (Ar) with at least one small *ortho* substituent, as well as Ar = biphenyl and Ar = naphthyl, has been synthesised. Crystallographic analyses of complexes **9** (Ar = 2,3-dimethylphenyl), **13** and **14** (Ar = biphenyl; X = Cl or Br, respectively) reveal a distorted trigonal-bipyramidal geometry in the solid state. These complexes, in combination with methyl aluminoxane (MAO), are active catalysts for the oligomerisation of ethylene, yielding >99% linear α-olefin mixtures that follow a Schulz–Flory distribution. Iron ketimine (R = Me) precatalysts give the highest activities and a greater α-value than their aldimine (R = H) analogues. Cobalt precatalysts follow a similar trend, though their activities are almost two orders of magnitude lower than those of the corresponding iron catalysts. Ethylene pressure studies on cobalt precatalyst **15** reveal a first-order dependence on ethylene for both the rate of propagation and the rate of chain transfer, and a pressure independence of the α value.

Keywords: cobalt · ethylene · iron · methylaluminoxane · N ligands · oligomerizations

Introduction

The oligomerisation of ethylene presents one of the major industrial processes for the production of linear α-olefins in the range C_6-C_{20}. Such linear oligomers are extensively used for the preparation of detergents, plasticizers and as comonomers in the polymerisation of ethylene to give linear low-density polyethylene (LLDPE). Originally linear α-olefins were manufactured by the Ziegler (Alfen) process which consists of a controlled ethylene growth reaction in the presence of triethylaluminium at 90–120 °C and at an ethylene pressure of 100 bar. α-Olefins are released from the aluminium centre at more elevated temperatures and lower pressures. Catalysts currently used in industry are either alkylaluminium compounds, a combination of alkylaluminium compounds with early transition metal compounds (e.g. titanium tetrachloride) or nickel(II) complexes with bidentate monoanionic [P,O] ligands (the SHOP process).[1, 2]

Nickel(II)-based catalysts with monoanionic [P,O] ligands (**A**, Figure 1) for the oligomerisation of ethylene have been extensively studied,[3–15] most notably by Keim et al.. Over the years many other monoanionic ligands have been investigated by Keim et al. and also by Cavell et al., for example [As,O],[16] [N,O],[17] [O,O],[18] [S,O][19, 20] and [S,S][19, 21–23] derivatives. In general, these monoanionic ligands result in neutral catalytically active alkyl or hydride species and require high reaction

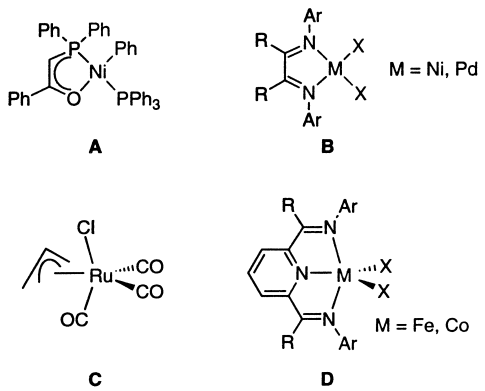

Figure 1. Examples of late transition metal oligomerisation catalysts.

[a] Prof. V. C. Gibson, Dr. G. J.P. Britovsek, Dr. S. Mastroianni, Dr. G. A. Solan, Dr. S. P. D. Baugh, Dr. C. Redshaw, Dr. A. J. P. White, Prof. D. J. Williams
Department of Chemistry
Imperial College
South Kensington, London SW7 2AY (UK)
Fax: (+44) 171-594-5810
E-mail: v.gibson@ic.ac.uk

[b] Dr. M. R. J. Elsegood
Department of Chemistry
Bedson Building, University of Newcastle
Newcastle upon Tyne NE1 7RU (UK)

  0947-6539/00/0612-2221 $ 17.50+.50/0

temperatures and pressure for the oligomerisation of ethylene; for example, the SHOP process operates at 80–120 °C and 70–140 bar.

Later, it was found that neutral [P,O] ligands, which afford cationic nickel complexes, oligomerise ethylene at much lower temperatures and pressures[24] and similar cationic palladium complexes dimerize ethylene to butene.[25] Recently various other neutral chelating ligands such as diimine [N,N] (**B**, Figure 1),[26–28] pyridylimine [N,N],[29–33] diamine [N,N][34] and iminophosphine [P,N][35] ligands have provided highly active nickel- and palladium-based oligomerisation catalysts.

In contrast to the high catalytic activity of Group 10 complexes as ethylene oligomerisation catalysts, very few active Group 8 or Group 9 oligomerisation catalysts have been reported. In the early days of homogeneous catalysis simple transition metal salts like $RuCl_3$ and $RhCl_3$ were reported to catalyse the dimerisation of ethylene under rather extreme conditions.[36, 37] Alkylaluminium activators and donor ligands were, however, found to improve the activity.[38] For the catalyst system $[Co(acac)_3]/AlEt_3$ (acac = acetylacetone) a selectivity for 1-butene of more than 99.5% was reported.[39] As the development of organometallic chemistry proceeded, hydrido[40–43] and σ-alkyl[44] transition metal complexes were employed, but still only dimers were obtained, indicating that in these catalyst systems the chain transfer process is very fast. The first oligomerisation of ethylene using a Group 8 metal complex was reported by Braca and Sbrana in 1974,[45] employing $[(\eta^3\text{-}C_3H_5)Ru(CO)_3Cl]$ as a catalyst (**C**, Figure 1). Ethylene was converted at 150 bar/180 °C to C_4–C_{14} olefins, albeit with low activity.

Recently ourselves, and Brookhart and Small have described highly active ethylene oligomerisation catalysts based on iron.[46, 47] The catalyst precursors contain neutral tridentate pyridyldiimine ligands with small substituents in the *ortho*-aryl position (**D**, Figure 1). Larger substituents result in the polymerisation of ethylene[47–52] and propylene.[53–55]

Herein we report a full discussion of our studies on this new oligomerisation system, demonstrating the differences between iron and cobalt precatalysts as well as the effects of different substituents on the aryl groups and the ligand backbone. Reaction parameters, such as pressure, temperature and co-catalyst concentration have also been investigated and their effect on activity, oligomer distribution and termination mechanism will be discussed. These results are complementary to those recently reported by Brookhart and Small.[46, 56]

Results

Synthesis and characterisation of ligands and complexes

Pyridyldiimine ligands **1**–**7** are conveniently prepared by condensation of 2,6-diacetylpyridine or 2,6-diformylpyridine with the corresponding aniline (Scheme 1).

Iron and cobalt complexes **8**–**17** of these ligands were prepared by dissolving anhydrous $FeCl_2$ or $CoCl_2$ in *n*-butanol at 80 °C, followed by addition of one equivalent of the ligand. After washing with diethyl ether, complexes **8**–**17** are obtained in good yield and in high purity.

Compared to analogous complexes with bulky substituents, these compounds with their smaller aryl substituents are significantly less soluble in hydrocarbon and polar solvents. The concentrations of saturated solutions in dichloromethane are too low for NMR spectroscopy.[57] However, some compounds could be recrystallised from hot acetonitrile. All of the compounds **8**–**17** are paramagnetic with magnetic moments for Fe typically between 4.9–5.5 μ_B and for Co about 4.6 μ_B, indicating quintet ($2S+1=5$) and quartet ($2S+1=4$) ground states, respectively. All complexes have been further characterised by FAB-MS and microanalysis. For compounds **9**, **13** and **14** X-ray structure analyses have been carried out, in the case of **9** using high flux synchrotron radiation due to the small size of the crystals.

The 2,3-dimethylphenylketimineiron complex **9** possesses a structure with approximate C_s symmetry about a plane containing the iron atom, the two chloro ligands and the pyridyl nitrogen atom (Figure 2). The solid-state structure is seen to be disordered with both "up" and "down" orientations of the two 2,3-dimethylphenyl rings (Figure 3), the dominant (ca. 75%) conformer being that illustrated in Figure 2. The

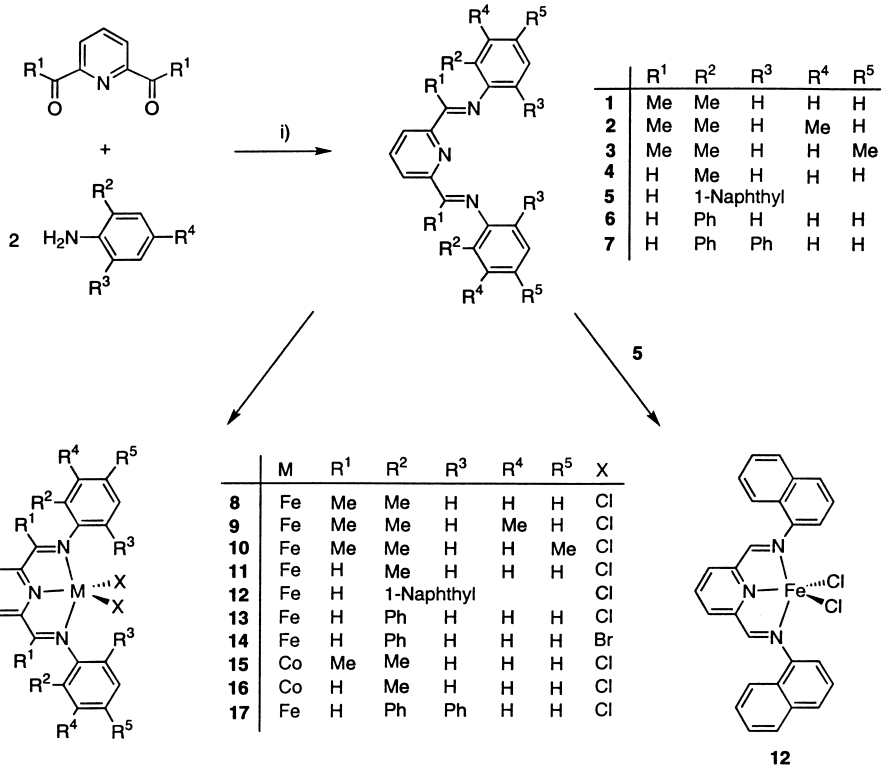

	R^1	R^2	R^3	R^4	R^5
1	Me	Me	H	H	H
2	Me	Me	H	Me	H
3	Me	Me	H	H	Me
4	H	Me	H	H	H
5	H	1-Naphthyl			
6	H	Ph	H	H	H
7	H	Ph	Ph	H	H

	M	R^1	R^2	R^3	R^4	R^5	X
8	Fe	Me	Me	H	H	H	Cl
9	Fe	Me	Me	H	Me	H	Cl
10	Fe	Me	Me	H	H	Me	Cl
11	Fe	H	Me	H	H	H	Cl
12	Fe	H	1-Naphthyl				Cl
13	Fe	H	Ph	H	H	H	Cl
14	Fe	H	Ph	H	H	H	Br
15	Co	Me	Me	H	H	H	Cl
16	Co	H	Me	H	H	H	Cl
17	Fe	H	Ph	Ph	H	H	Cl

Scheme 1.

0947-6539/00/0612-2222 $ 17.50+.50/0 *Chem. Eur. J.* **2000**, *6*, No. 12

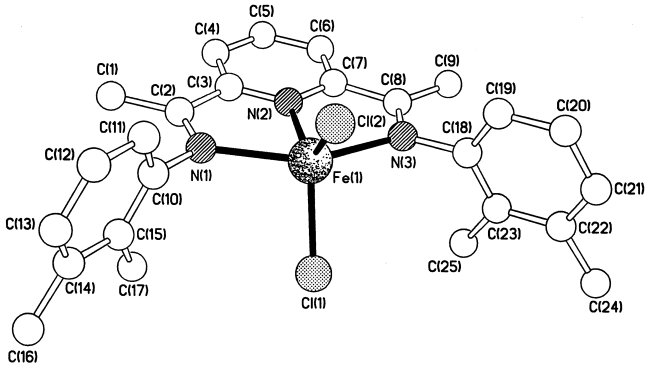

Figure 2. The molecular structure of the dominant conformation present in the crystals of **9**.

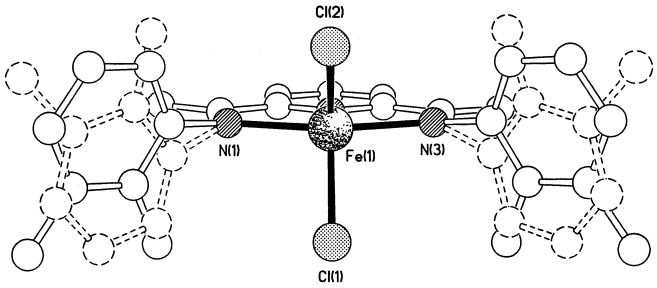

Figure 3. The "up"/"down" disorder of the 2,3-dimethylphenyl rings in the structure of **9**.

two dimethylphenyl rings are oriented almost orthogonally (ca. 81°) to the pyridyldiimine plane. The atoms comprising this latter plane are coplanar to within 0.021 Å, the iron atom deviating by only 0.022 Å from this plane (Figure 4). Within

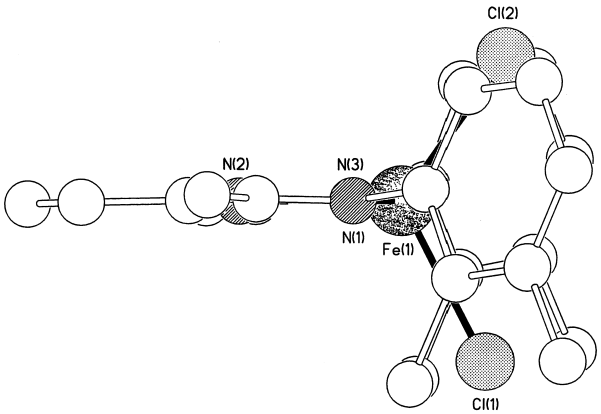

Figure 4. Parallel projection down the N(1)···N(3) vector of the tridentate ligand in **9** showing the in-plane location of the iron atom.

the ligand there is no evidence of any bond delocalisation involving the imines, the two C=N bonds having clear double-bond character (1.278(3) and 1.280(3) Å). The geometry at the iron centre is probably best described as distorted trigonal bipyramidal with the pyridyl nitrogen atom and the two chloro ligands forming the equatorial plane. The equatorial angles range between 116.49(2) and 126.27(5)° and the two axial Fe–N bonds subtend an angle of 146.88(6)°, a distortion that is a consequence of satisfying the tridentate chelating constraints of the ligand (Table 1). The two axial Fe–N bond

Table 1. Selected bond lengths [Å] and angles [°] for **9**.

Fe(1)–N(1)	2.2166(17)	Fe(1)–N(2)	2.0995(16)
Fe(1)–N(3)	2.2148(17)	Fe(1)–Cl(1)	2.3018(7)
Fe(1)–Cl(2)	2.2741(7)	N(1)–C(2)	1.280(3)
N(3)–C(8)	1.278(3)		
N(2)-Fe(1)-N(1)	73.55(6)	N(3)-Fe(1)-N(1)	146.88(6)
N(1)-Fe(1)-Cl(1)	97.84(5)	N(1)-Fe(1)-Cl(2)	99.61(5)
N(2)-Fe(1)-N(3)	73.33(6)	N(2)-Fe(1)-Cl(1)	117.24(5)
N(2)-Fe(1)-Cl(2)	126.27(5)	N(3)-Fe(1)-Cl(1)	97.47(5)
N(3)-Fe(1)-Cl(2)	99.52(5)	Cl(2)-Fe(1)-Cl(1)	116.49(2)

lengths, 2.217(2) and 2.215(2) Å are, as expected, longer than those to the pyridyl nitrogen atom (2.100(2) Å), a geometry similar to that observed in the bis(2,6-diisopropylphenylimino)pyridyl derivatives,[47, 52] but with a significant shortening of the two axial bonds commensurate with the in-plane positioning of the iron atom, see, for example, the out of plane geometry observed in the 2,6-diisopropyl analogue. There is a significant asymmetry in the two Fe–Cl linkages, with that to Cl(1) being about 0.028 Å longer than that to Cl(2), a difference virtually identical to that seen in the 2,6-diisopropyl complex. In this latter complex, the difference was attributed to the pseudo-square-pyramidal geometry where the longer Fe–Cl bond was associated with the apical site. A similar argument could be applied to **9** since the largest departure from trigonal-bipyramidal geometry is associated with the N(2)-Fe(1)-Cl(2) angle (126.3(1)°), which would make Cl(1) the apical atom of a very severely distorted square based pyramid. There are no noteworthy intermolecular packing interactions.

The $FeCl_2$ and $FeBr_2$ 2-biphenylaldimine complexes, **13** and **14**, respectively, are isomorphous, both having approximate C_s symmetry about a plane containing the two halogens, the pyridyl nitrogen atom and the metal centre (Figure 5). As the

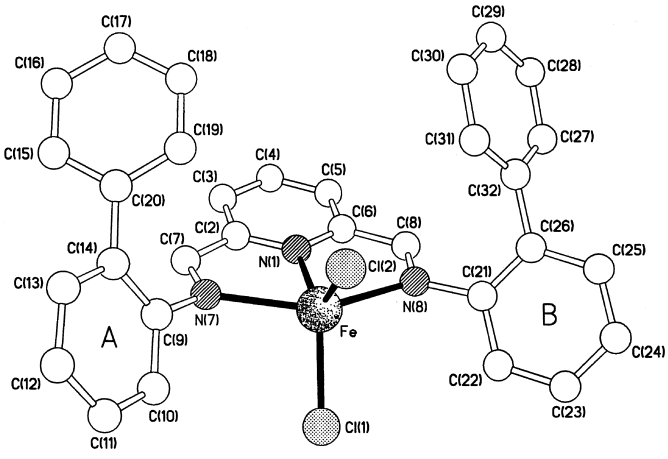

Figure 5. The molecular structure of **13** (that of **14** is isomorphous).

only significant difference between the two complexes is in the iron–halogen distances (vide infra), we will restrict our discussion to the chloride complex, giving the values for the bromide complex in parentheses; selected bond lengths and angles are collected in Table 2. The pyridyldiimine unit is coplanar to within 0.036 Å (0.049 Å), the iron atom lying only 0.049 Å (0.057 Å) out of this plane (Figure 6). The two imino

Table 2. Selected bond lengths [Å] and angles [°] for **13** and **14**.

	13 (X = Cl)	**14** (X = Br)		**13** [X = Cl]	**14** (X = Br)
Fe–N(1)	2.108(5)	2.108(7)	Fe–N(7)	2.263(5)	2.243(8)
Fe–N(8)	2.266(5)	2.265(8)	Fe–X(1)	2.304(2)	2.451(2)
Fe–X(2)	2.273(2)	2.414(2)	C(7)–N(7)	1.279(8)	1.292(12)
C(8)–N(8)	1.282(8)	1.266(12)			
N(1)-Fe-N(7)	73.4(2)	73.4(3)	N(1)-Fe-N(8)	73.2(2)	73.3(3)
N(1)-Fe-X(1)	119.4(2)	117.3(2)	N(1)-Fe-X(2)	124.0(2)	125.5(2)
N(7)-Fe-N(8)	146.5(2)	146.4(3)	N(7)-Fe-X(1)	98.4(2)	98.2(2)
N(7)-Fe-X(2)	99.0(2)	98.4(2)	N(8)-Fe-X(1)	100.3(2)	100.4(2)
N(8)-Fe-X(2)	97.2(2)	97.7(2)	X(1)-Fe-X(2)	116.56(9)	117.19(7)

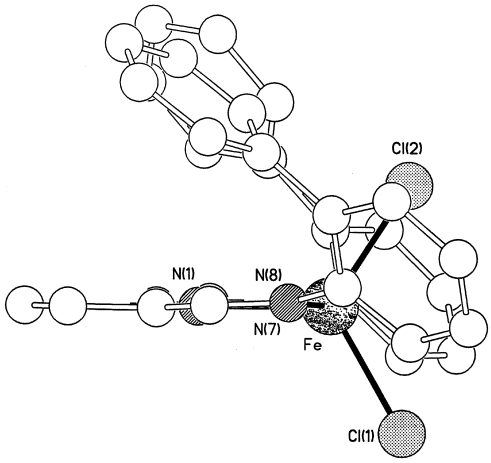

Figure 6. Side view of the structure of **13** viewed down the N(7)···N(8) vector, showing the in-plane geometry of the iron centre.

C=N double bonds have distinctive double-bond character with C–N distances of 1.279(8) and 1.282(8) Å (1.266(12) and 1.292(12) Å). The phenyl rings **A** and **B** are rotated by 58 and 55° (55 and 55°) respectively out of the plane of the ligand backbone, and each biphenyl unit has a distinctly twisted conformation with a twist angle of 56° (54°) associated with the unit containing ring **A**, and 64° (64°) with that containing ring **B**. The geometry at iron is distorted trigonal bipyramidal with equatorial angles ranging between 116.6(1) and 124.0(2)° (117.2(1) and 125.5(2)°) and the "axial" Fe–N bonds subtend an angle of 146.5(2)° (146.4(3)°). As in **9**, the two axial bond lengths are the same, both being longer than that to the pyridyl nitrogen atom. There is also a similar asymmetry in the iron-halide distances with that to X(1) in the pseudo apical position of the severely distorted square-based pyramid (vide supra) being longer by about 0.031 Å (0.037 Å) than that to the "basal" halogen X(2). Inspection of the packing of the molecules does not reveal any intermolecular interactions of note other than normal van der Waals.

Oligomerisation results

General: The catalytic activity of precatalysts **8**–**16** presented in Scheme 1 for the oligomerisation of ethylene has been evaluated employing methylaluminoxane (MAO) as co-catalyst. The catalysts display similar activation characteristics to those observed for the analogous polymerization systems,[52] that is an immediate exotherm results with no induction period. During the oligomerisation reaction (1 h) a decrease in activity is noticed, the final activity being typically 10–20% of the initial activity.

Oligomerisation conditions and results are presented in Table 3. Iron catalysts were tested at 5 bar ethylene pressure and 50 °C for 1 h, using 100 equivalents of MAO as the co-catalyst and 900 equivalents of MAO as the scavenger. Cobalt catalysts (**15** and **16**) displayed relatively low activities under these conditions (see run 6, Table 3). For this reason, cobalt catalysts were tested at 10 bar of ethylene pressure, while keeping catalyst and co-catalyst concentrations the same as for the Fe catalysts. Catalyst activities were calculated from the GC traces, using extrapolated values for C_4–C_8 (see Experimental Section).

Ligand and metal effects: All of the iron complexes, except the *ortho*-phenyl aldimine derivatives **13** and **14**, are highly active for the oligomerisation of ethylene. Iron ketimine catalysts **8**–**10** gave the highest activities, generally exceeding 1000 gmmol^{-1}h^{-1}bar^{-1} under the conditions employed here. Methyl substituents in *meta* and *para* positions on the aryl rings affect the activities significantly (see runs 1–3 in Table 3), whereby the *meta* methyl-substituted precatalyst **9**

Table 3. Ethylene oligomerisation results from precatalysts **8**–**16**.[a]

Run	Precat. [μmol]	MAO [equiv]	*P* [bar]	*T* [°C]	Yield[c] [g]	Activity [g mmol^{-1}h^{-1}bar^{-1}]	α	β	M_n[d]	M_w[d]	M_w/M_n[d]
1	**8** (6)	1000	5	50	38.9	1300	0.79	0.26	700	1500	2.1
2	**9** (6)	1000	5	50	77.2	2570	0.79	0.27	600	2700	4.7
3	**10** (6)	1000	5	50	31.3	1040	0.78	0.29	700	1900	2.8
4	**11** (6)	1000	5	50	14.4	480	0.50	1.00			
5	**12** (6)	1000	5	50	6.88	230	0.63	0.58			
6	**15** (6)	1000	5	50	0.69	23	0.67	0.48			
7	**15** (6)	1000	10	50	1.56	26	0.63	0.60			
8	**15** (6)	1000	15	50	4.47	50	0.66	0.51			
9	**15** (6)	1000	10	35	1.79	30	0.72	0.39			
10	**15** (6)	1000	10	70	0.76	13	0.53	0.87			
11	**16** (6)	1000	10	50	0.43	7	0.74	0.35			
12[b]	**8** (2)	100	5	50	20.1	2010	0.73	0.37			
13[b]	**9** (2)	100	5	50	41.7	4170	0.77	0.29			
14[b]	**10** (2)	100	5	50	26.6	2660	0.70	0.42			

[a] Isobutane solvent, reaction time 1 h; MAO scavenger (900 equiv). [b] Triisobutylaluminium scavenger (2 mmol, 1000 equiv). [c] Determined from GC, using extrapolated values for C_4–C_8. [d] Toluene-insoluble fraction, determined by GPC at 135 °C.

0947-6539/00/0612-2224 $ 17.50+.50/0 *Chem. Eur. J.* **2000**, *6*, No. 12

shows the highest activity (2570 $gmmol^{-1}h^{-1}bar^{-1}$). Similar trends are seen under slightly different conditions, that is lower catalyst and MAO concentrations and triisobutylaluminium as the scavenger (runs 12–14, Table 3), though interestingly, under these conditions higher catalyst activities are found. In addition to the toluene-soluble fraction of oligomers, catalysts **8**–**10** also yield a toluene-insoluble PE fraction, which was shown by GPC and NMR spectroscopy to consist of higher molecular weight ($> C_{30}$) α-olefins ($M_n = 700$ corresponds to C_{50}). The activity of the cobalt ketimine complex **15** is substantially less than for its iron analogue **8** (compare runs 1 and 6 in Table 3), a trend that parallels the behaviour of iron versus cobalt ethylene polymerisation catalysts, though the difference is more pronounced for the oligomerisation systems.[47, 49, 52]

The activity of the *ortho*-methyl iron aldimine catalyst **11** is approximately one third of the activity of its ketimine counterpart **8**, in keeping with the trends observed for ketimine versus aldimine polymerisation catalysts. Iron aldimine catalyst **12** with 1-naphthyl substituents gave a further reduction in activity, while iron aldimine complexes **13** (dichloride) and **14** (dibromide), containing 2-biphenyl substituents, only yielded trace amounts of oligomers under the conditions used here. The crystal structures of complexes **13** and **14** do not reveal any obvious explanations for their anomalous behaviour. Significantly, complex **17**, with two *ortho*-phenyl substituents also gives an unusually low activity as a polymerisation catalyst. The reason for the different effect of *ortho*-aryl versus *ortho*-alkyl substituents is unclear at this stage but may involve deactivation of the catalyst by intramolecular C–H activation of the *ortho*-phenyl substituents. The cobalt aldimine complex **16**, with an activity of only 7 $gmmol^{-1}h^{-1}bar^{-1}$ follows the general trend in activity seen for iron versus cobalt and ketimine versus aldimine catalysts.

In all cases the catalysts give a Schulz–Flory distribution of oligomers, which can be quantified by the α value. The α value represents the probability of chain propagation and is experimentally determined by the mole ratio of two oligomer fractions, C_{14} and C_{12} in this case [Eq. (1)].

$$\alpha = \frac{\text{rate of propagation}}{\text{rate of propagation} + \text{rate of chain transfer}} = \frac{\text{moles of } C_{n+2}}{\text{moles of } C_n} \quad (1)$$

$$\beta = \frac{\text{rate of chain transfer}}{\text{rate of propagation}} = \frac{1-\alpha}{\alpha} \quad (2)$$

An illustration of the differing oligomer distributions is shown in Figure 7, the yield of each fraction being plotted against the carbon number for the iron ketimine (**8**) versus aldimine (**11**) catalysts. From Figure 7 it can be seen that for an α value of 0.8 the weight fraction is at a maximum for C_8, and for $\alpha = 0.5$ the weight maximum is at C_4. The α and β values characteristic for the distribution of oligomers obtained with precatalysts **8**–**16** are given in Table 3.

Unlike the differences in activity observed for iron ketimine complexes **8**–**10**, additional methyl groups in the *meta* and *para* position on the aryl ring substituents have very little effect on the α value (runs 1–3, Table 3). Whereas the differences in activity are most likely due to an electronic

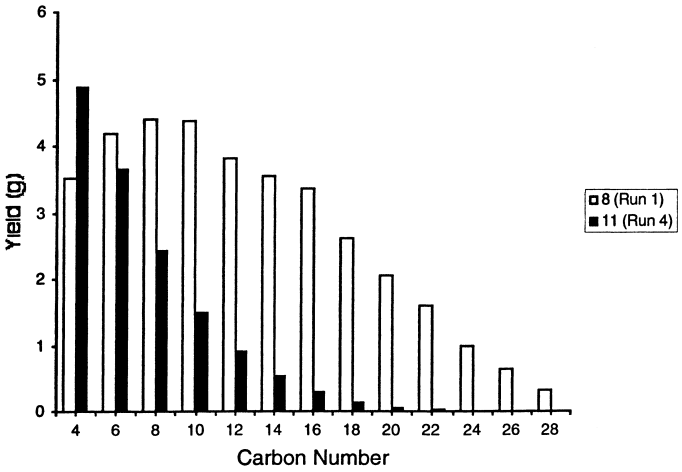

Figure 7. Oligomer distribution: yield of each oligomer fraction versus carbon number.

effect, the α value seems to be more sensitive to steric effects. This is also seen when comparing ketimine catalysts with the less sterically hindered aldimine catalysts. Aldimine precatalyst **11** with *o*-methylphenyl substituents gives an α value of 0.50 for the oligomer distribution (run 4, Table 3, in this case $\beta = \text{rate}_{trans}/\text{rate}_{prop} = 1.00$), whereas aldimine precatalyst **12**, with the larger 1-naphthyl substituents gives an α value of 0.63. The effect of different ligands and metal centres on the α value is illustrated in Figure 8, which shows the ln mol% versus the carbon number of the oligomers for complexes **8**, **11** and **15** (runs 1, 4 and 6, Table 3). The less active cobalt

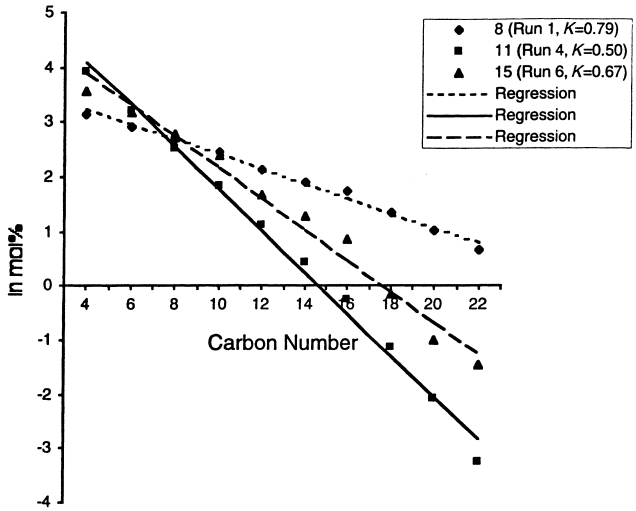

Figure 8. Schulz–Flory distribution: ln mol% of each fraction versus carbon number.

ketimine catalyst **15** gives a lower α value of 0.67 compared with 0.79 for the analogous iron complex under these conditions. The value of 0.70 for the cobalt aldimine catalyst **16** is somewhat inconsistent, but this value is subject to a large error due to the very low activity observed for this catalyst (only 0.43 g oligomers in 400 mL toluene).

Overall, the trends in oligomerisation activities and oligomer distributions observed with the various types of

catalysts studied here, that is iron and cobalt with ketimine and aldimine ligands, parallel the trends observed in the ethylene polymerisation systems. Iron ketimine precatalysts give the highest α values and highest activities, followed by the aldimine analogues which give lower molecular weight products and about half the activity. The cobalt systems are at least an order of magnitude less active and molecular weights and α values are intermediate between those obtained for iron ketimine and aldimine systems.

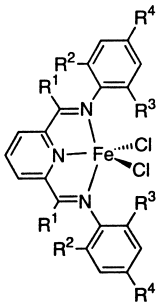

		R^1	R^2	R^3	R^4
[1]	**8**	Me	Me	H	H
	18	Me	Me	Me	H
[2]	**10**	Me	Me	H	Me
	20	Me	Me	Me	Me
[3]	**11**	H	Me	H	H
	19	H	Me	Me	H
[4]	**13**	H	Ph	H	H
	17	H	Ph	Ph	H

Figure 9. Four sets of precatalysts with one and two ortho substituents.

Discussion

The role of the aryl substituents: During the past five years an interesting significance has emerged for ligands containing bulky aryl substituents. In olefin polymerisation catalysis, monodentate, bidentate and tridentate ligands containing bulky aryl substituents have been used across the transition series, resulting in the formation of high molecular weight polyolefins. Examples of this kind can be found for dianionic bidentate[58–64] and tridentate[65–69] diamide ligands in Group 4 metal catalysts, monoanionic bidentate ligands for Groups 4 and 6,[70, 71] and neutral bidentate ligands for Group 10 metal catalysts.[31, 72–77]

In some cases, the molecular weight of the resulting polymer product was found to be related to the steric bulk of the aryl substituents, whereby increased size results in higher molecular weight polyolefins.[62, 72, 76, 78] Such correlation also appears for iron and cobalt pyridyldiimine systems. The steric and electronic properties of substituents on the aryl rings, as well as the number and the position (*ortho*, *meta* or *para*) of these substituents can have a dramatic effect on the catalytic activity of the precatalysts and the properties of the polymer/oligomer product. In particular, substituents in the ligand backbone and the *ortho* position of the aryl rings have a marked effect on the molecular weight of the product and the catalytic activity. As reported previously, substituents in both *ortho* aryl positions result in the formation of high molecular weight polyethylene, and the PE molecular weight is dependent upon the size of these substituents.[52]

Comparing precatalysts containing one versus two *ortho* substituents, as shown in Figure 9, we see even larger variations in the molecular weight of the polyethylene products and also the activity of the catalysts. From Table 4 it can be seen that the two ketimine sets [1] [2-methyl (**8**) and 2,6-dimethyl (**18**)] and [2] [2,4-dimethyl (**10**) and 2,4,6-trimethyl (**20**)] show a dramatic increase in molecular weight and activity, when going from one to two *ortho* methyl substituents. A similar increase in molecular weight is observed for the aldimine set [3] [2-methyl (**11**) versus 2,6-dimethyl (**19**)], although the effect on activity is less pronounced. The *ortho*-phenyl aldimine precatalysts, **13** and **17** in set [4] give significantly lower productivities, and the 2,6-diphenyl derivative affords low molecular weight polyethylene. The activity of the *ortho* phenyl-substituted aldimine catalyst **13** was too low to allow meaningful product analysis. However, given the lower molecular weight product of the diphenyl-substituted derivative **17**, **13** is expected to give very low molecular weight oligomers under optimised conditions. Overall, activities for mono-substituted derivatives are generally lower, and oligomeric products are obtained instead of polymer. We can summarize by arranging the mono-*ortho* substituted precatalysts in the following series, whereby the molecular weight and the activity reduces in the order: *t*Bu[52] > *i*Pr[46] > Me > Ph and ketimine > aldimine. Interestingly, this order correlates well with a pattern observed by McConville and co-workers for related pyridyldiamidozirconium complexes.[79] Rotation around the nitrogen – aryl bond in a series of zirconium complexes containing substituents in the *ortho*-aryl position, was studied by using variable-temperature NMR techniques, and was found to decrease in the order *t*Bu > Me > Ph. Brookhart and Small have already shown[53] that a similar restricted rotation occurs in pyridyldiimine ligands and we conclude that in iron and cobalt pyridyldiimine complexes restricted rotation around the nitrogen – aryl bond is the key factor responsible for high molecular weight product. Unfortunately, the paramagnetic nature of these iron and cobalt complexes precludes a detailed NMR investigation of the barriers to aryl group rotation.

Table 4. Comparative study between precatalysts containing one and two *ortho* substituents.

Set	Run	Precat. [μmol]	MAO [equiv]	*P* [bar]	*T* [°C]	Yield[c] [g]	Activity [g mmol^{-1} h^{-1} bar^{-1}]	α	β	M_n[c]	M_w[c]	M_w/M_n[c]
[1]	1	**8** (6)	1000	5	50	38.9	1300	0.79	0.26	700	1500	2.1
[1]	15[b]	**18** (0.6)	1000	10	50	56.5	9340			9600	242000	25.3
[2]	3	**10** (6)	1000	5	50	31.3	1040	0.78	0.29	700	1900	2.8
[2]	16[b]	**20** (0.6)	1000	10	50	123.5	20600			14000	148000	10.7
[3]	4	**11** (6)	1000	5	50	14.4	480	0.50	1.00			
[3]	17	**19** (6)	1000	5	50	18.2	610			1500	31000	21.4
[4]	18	**13** (6)	1000	5	50	trace	< 1					
[4]	19	**17** (6)	1000	5	50	1.25	42			690	1200	1.8

[a] Isobutane solvent, reaction time 1 h; MAO scavenger. [b] Triisobutylaluminium scavenger. [c] Determined by GPC at 135 °C.

0947-6539/00/0612-2226 $ 17.50+.50/0 *Chem. Eur. J.* **2000**, *6*, No. 12

Pressure and temperature effects: Pressure variation studies on ethylene polymerisation catalysts such as the 2,6-diisopropylphenyl ketimine iron and cobalt precatalysts have shown in both cases a first-order dependence of the productivity on ethylene pressure.[52] In addition, the polymer molecular weight was found to be invariant with respect to ethylene pressure. These findings are explained by a first-order dependence on ethylene concentration both for the rate of propagation and the rate of chain transfer by β-hydrogen transfer. Brookhart and Small have shown for the *ortho*-methyl ketimine iron complex **8** a first-order dependence of the rate of propagation on ethylene concentration and the α value was found to be invariant with ethylene pressure, indicating also that chain transfer is first order in ethylene.[46] The effect of ethylene pressure on the activity and oligomer distribution has been studied here for the structurally analogous cobalt precatalyst **15**. A similar first order dependence for the rate of propagation is observed, although at higher pressure some deviation is observed (runs 6–8, Table 3), which may be explained by the larger error in the activity determination. The α value remains fairly constant during these runs, indicating an ethylene pressure independence of α for cobalt complex **15**. We can therefore quite confidently conclude that, within the conditions employed, for all iron and cobalt pyridyldiimine catalysts studied so far, both oligomerisation and polymerisation catalysts, the rate of propagation and the rate of β-H transfer are first order in ethylene.

Experiments in which the temperature of the polymerization reaction was varied for cobalt precatalyst **15** (runs 9, 7 and 10, Table 3) reveal that an increase in temperature results in a decrease in productivity and the α factor. Elevated temperatures are expected to result in overall higher propagation and transfer rates and therefore higher productivities. As the dependence of α with temperature indicates, the rate of chain transfer increases more than the rate of propagation which is expected to afford lower molecular weight products. However, there are two counter-effects to this that are likely to be operating. Firstly, a decrease in ethylene solubility at higher temperatures[80, 81] (i.e. lower monomer concentrations) will lead to reduced productivity, and secondly higher temperatures can result in higher rates of catalyst deactivation. It is a combination of these effects that is likely to account for the observed temperature dependence of the productivity. The decrease of the α value at higher temperature is consistent with the observations made for iron complex **8** by Brookhart and Small[46] and for nickel(II) α-diimine oligomerisation catalysts.[26]

Chain transfer mechanism: Analysis by GC/MS of the oligomerisation products reveal product selectivities for linear α-olefins, under the conditions used here, greater than 99% in all cases. Neither branched oligomers nor isomerisation to internal olefins is observed. This high selectivity, combined with a Schulz–Flory oligomer distribution, is consistent with an oligomerisation mechanism starting from an alkyl species, which is formed from the dichloro precatalyst and the co-catalyst MAO, followed by several insertions of ethylene (propagation) and a chain transfer process. Chain propagation proceeds by coordination and migratory insertion of ethylene into the metal–alkyl bond and is first order in ethylene. After a number of insertions (generally less than 15) a transfer process will eliminate the α-olefin product from the metal centre and regenerate the active species. Unlike the polymerisation of ethylene, the formation of rather short oligomer chains means that the rate of chain transfer has become competitive with the rate of chain propagation (see run 4 in Table 3, where $\alpha = 0.50$ and $\beta = \text{rate}_{trans}/\text{rate}_{prop} = 1.00$). From experiments presented here and results by Brookhart on complex **8**, the α factor is pressure independent, indicating that also the chain transfer process is first order in ethylene. Similar results have been obtained for the related ethylene polymerisation systems, where the polymer molecular weight is pressure independent.[52]

For late transition metal ethylene oligomerisation catalysts, chain transfer generally implies a β-hydrogen transfer process and the formation of an α-olefin. For iron and cobalt oligomerisation catalysts we have established a first-order ethylene dependence of the rate of chain transfer. Four different transfer processes are considered in Scheme 2. From a cationic alkyl species, chain transfer may occur through an associative displacement mechanism (**A**), in which the β-hydrogen atom is transferred to the metal, generating a metal hydride species. This process is also referred to as monomer-assisted β-hydrogen elimination. An alternative pathway, kinetically indistinguishable from **A** (both pathways are first order in ethylene) is β-hydrogen transfer to monomer (**B**) in which the β-hydrogen atom is directly transferred onto the incoming monomer, without any interaction with the metal. This alternative process has been postulated previously for metallocene polymerisation catalysts[82–85] and calculations suggest its involvement in late transition metal systems,[86] though experimental verification has not been obtained to date. A third possible termination process, mentioned here for completeness, is by σ-bond metathesis (pathway **C**, Scheme 2). This transfer mechanism involves transfer of a hydrogen atom of the monomer, ethylene in this case, to the growing polymer chain and the generation of an iron–vinyl species, which can restart chain growth. The vinyl end-group is in this case introduced at the beginning of the polymer chain. The involvement of σ-bond metathesis as a possible transfer mechanism has been observed for Group 4[87–89] and Group 3 metallocenes[90–92] and constrained geometry catalyst systems.[93, 94] Either **A**, **B** or **C** is the dominant chain transfer pathway in these iron and cobalt oligomerisation systems.

For iron-based polymerisation systems an additional transfer process, chain transfer to aluminium (**D** in Scheme 2) is observed, in particular at low ethylene pressure (1 bar).[52] At lower ethylene concentrations, the rate of the β-hydrogen transfer process is reduced and this chain transfer to aluminium process becomes competitive, yielding besides vinyl end-capped polymer also saturated polymer chains. These saturated products arise from a chain transfer process with trimethylaluminium, present in MAO which is used as the co-catalyst. However, chain transfer to aluminium is not observed with any of the oligomerisation systems studied here. An oligomerisation run at 1 bar ethylene pressure, using

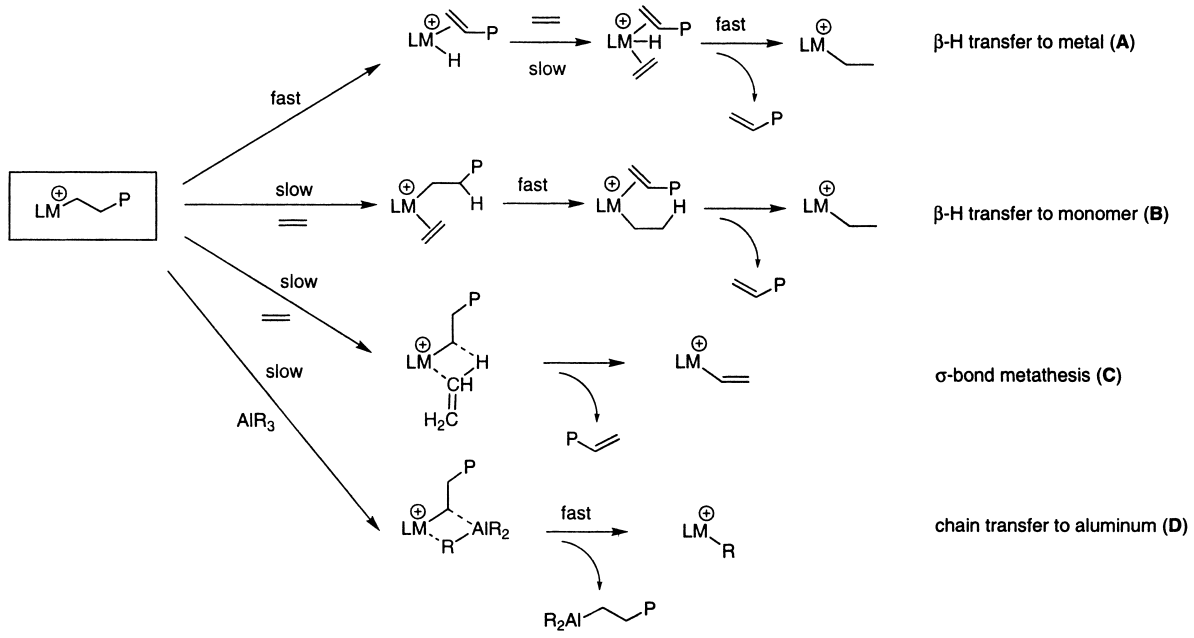

Scheme 2.

precatalyst **11** and 1000 equivalents of MAO, yielded no saturated alkane products. For these oligomerisation systems, the higher β-hydrogen transfer rate ensures that β-hydrogen transfer is the dominant transfer process, even in the presence of a relatively high concentration of alkyl aluminium. Alternatively, one could conclude that chain transfer to aluminium occurs more readily with catalysts that contain more sterically demanding ligands.

Noteworthy, some catalyst systems are deactivated in the presence of a large excess of certain alkylaluminium reagents used as scavengers. For example, iron aldimine precatalyst **11** and the cobalt complexes **15** and **16** are deactivated when triisobutylaluminium (900 equiv) is used as a scavenger. These results seem to indicate that catalytic intermediates formed from precursors containing pyridyldiimine ligands lacking sufficient steric bulk in the *ortho*-aryl position and the ligand backbone, are more easily deactivated through an interaction or reaction with the alkylaluminium reagent.

Conclusion

We have shown that iron and cobalt bis(imino)pyridyl complexes containing imino-aryl rings with one small *ortho* substituent, especially methyl, can be activated with MAO to give ethylene oligomerisation catalysts. The activity is strongly affected by the metal centre and to a lesser extent by the ligand backbone, resulting in the following activity order of merit: Fe/ketimine > Fe/aldimine $\gg$ Co/ketimine > Co/aldimine. This order parallels the general trend observed for related polymerisation systems. The oligomer distribution factor α is more sensitive to the ligand architecture (ketimine vs. aldimine) than to the metal centre (iron vs. cobalt). Additional methyl substituents in the *meta*- or *para*-positions of the aryl rings increase the activity, but have very little effect on the α-value. α-Naphthyl and biphenyl substituents on the imino nitrogen donor also result in oligomerisation systems, the latter with very low activity. Significantly, the iron and cobalt oligomerisation systems presented here are highly selective for the formation of linear α-olefins with no branching or isomerisation to internal olefins being observed. This remarkable selectivity implies that the only chain transfer process operating with these systems is β-H transfer. Although some of the oligomerisation systems described have shown a sensitivity towards certain alkylaluminium reagents, no chain transfer to aluminium is observed, in contrast to related polymerisation systems. In conclusion, these results reinforce the importance of ligand architecture in bis(imino)-pyridyliron and -cobalt catalysts, in particular the role of steric effects at the *ortho*-aryl and imine carbon positions. Studies into the effects of varying the electronic nature of substituents attached to the aryl rings are presently in progress and will be reported in due course.

Experimental Section

General: All manipulations were carried out under an atmosphere of nitrogen using standard Schlenk and cannula techniques or in a conventional nitrogen-filled glove-box. Solvents were refluxed over an appropriate drying agent, and distilled and degassed prior to use. Elemental analyses were performed by the microanalytical services of the Department of Chemistry at Imperial College and Medac Ltd. NMR spectra were recorded on a Bruker spectrometer at 250 MHz (^{1}H), and 62.9 MHz (^{13}C) at 293 K; chemical shifts are referenced to the residual protio impurity of the deuterated solvent. Mass spectra were obtained using either fast atom bombardment (FAB), electron ionisation (EI) or chemical ionization (CI). Magnetic Susceptibility studies were performed using an Evans balance. Oligomer products were analysed by GC/MS, using a 25m BPX-5 column, injector temperature 240 °C and the following temperature programme: 100 °C/10 min, 100 – 320 °C/12 °C min^{-1}, 320 °C/10 min. The individual products were identified by MS (Micromass Autospec-Q) and integrated, using *n*-heptane as internal standard.

Materials: 2,6-Pyridinedicarboxaldehyde[95], 2,6-diphenylaniline[96] and precatalysts **18**, **19** and **20**[52] were prepared according to established

0947-6539/00/0612-2228 $ 17.50+.50/0 *Chem. Eur. J.* **2000**, *6*, No. 12

procedures, while 2,6-diacetylpyridine, MAO (10% solution in toluene) and all other anilines were purchased from Aldrich Chemical Co. All other chemicals were obtained commercially and used as received unless stated otherwise.

Synthesis of ligands

2,6-bis[1-(2-methylphenylimino)ethyl]pyridine (1): *o*-Toluidine (1.23 g, 2.5 equiv) was added to a solution of 2,6-diacetylpyridine (0.54 g, 3.31 mmol) in absolute ethanol (20 mL). After the addition of two drops of acetic acid (glacial) the solution was refluxed overnight. Upon cooling to room temperature the product crystallised from ethanol. The product was filtered, washed with cold ethanol and dried in a vacuum oven (50 °C) overnight. Yield: 33%. ^{1}H NMR ($CDCl_3$): $\delta = 8.48$ (d, 2H; pyrH), 7.91 (t, 1H; pyrH), 7.28 (m, 4H; ArH), 7.10 (m, 2H; ArH), 6.75 (m, 2H; ArH), 2.42 (s, 6H; $ArCH_3$), 2.20 (s, 6H; N=CCH_3); ^{13}C NMR ($CDCl_3$): $\delta = 166.82$, 155.40, 149.94, 136.79, 130.41, 127.08, 126.41, 123.59, 122.26, 118.14, 17.77 ($ArCH_3$), 16.29 (N=CCH_3); elemental analysis calcd for $C_{23}H_{23}N_3$: C 80.90, H 6.79, N 12.30; found: C 81.16, H 6.80, N 12.35.

2,6-bis[1-(2,3-dimethylphenylimino)ethyl]pyridine (2): Procedure as for **1**. Yield: 80%. ^{1}H NMR ($CDCl_3$): $\delta = 8.41$ (d, 2H; pyrH), 7.89 (t, 1H; pyrH), 7.10, 6.94, 6.55, (m, 6H; ArH, pyrH), 2.33 (s, 12H; N=CCH_3 and $ArCH_3$), 2.05 (s, 6H; $ArCH_3$); ^{13}C NMR ($CDCl_3$): $\delta = 166.70$, 155.44, 149.85, 137.51, 136.76, 125.73, 125.57, 125.17, 122.18, 115.99, 20.27 (m-CH_3), 16.29 (N=CCH_3), 13.79 (o-CH_3); mass spectrum: *m/z* : 369 $[M]^+$; elemental analysis calcd for $C_{25}H_{27}N_3$: C 81.30, H 7.32, N 11.38; found: C 81.71, H 7.67, N 11.11.

2,6-bis[1-(2,4-dimethylphenylimino)ethyl]pyridine (3): Procedure as for **1**. Yield: 75%. ^{1}H NMR ($CDCl_3$): $\delta = 8.42$ (d, 2H; pyrH[3]), 7.89 (t, 1H; pyrH[4]), 7.05 (m, 4H; ArH), 6.62 (d, 2H; ArH), 2.37 (s, 6H; N=CCH_3), 2.36 (s, 6H; *p*-CH_3), 2.13 (s, 6H; o-CH_3); ^{13}C NMR ($CDCl_3$): $\delta = 166.86$, 155.52, 147.38, 136.71, 132.93, 131.11, 127.07, 126.89, 122.15, 118.11, 20.83 (*p*-CH_3), 17.73 (*o*-CH_3), 16.23 (N=CCH_3); mass spectrum: *m/z*: 369 $[M]^+$; elemental analysis calcd for $C_{25}H_{27}N_3$: C 81.30, H 7.32, N 11.38; found: C 82.01, H 7.79, N 11.05.

2,6-bis[(2-methylphenylimino)methyl]pyridine (4): o-Toluidine (7.73 g, 2.5 equiv) was added to a solution of 2,6-diformylpyridine (3.90 g; 29 mmol) in absolute ethanol (20 mL) at room temperature. The product precipitated immediately and the mixture was stirred at room temperature for one hour. The product was filtered, washed with cold ethanol and dried in a vacuum oven (50 °C) overnight. Beige solid; yield: 70%. ^{1}H NMR ($CDCl_3$): $\delta = 8.60$ (s, 2H; N=CH), 8.35 (d, 2H; pyrH[3]), 7.95 (t, 1H; pyrH[4]), 7.26–7.05 (m, 8H; ArH), 2.43 (s, 6H; $ArCH_3$); ^{13}C NMR ($CDCl_3$): 159.37, 154.82, 149.87, 137.21, 132.45, 130.45, 126.84, 126.57, 122.89, 117.54, 17.89 ($ArCH_3$); elemental analysis calcd for $C_{21}H_{19}N_3$: C 80.48, H 6.11, N 13.40; found: C 80.61, H 6.14, N 13.48.

2,6-bis[(1-naphthylimino)methyl]pyridine (5): Procedure as described for **1**. Yellow solid; yield: 80%. ^{1}H NMR ($CDCl_3$): $\delta = 8.81$ (s, 2H; N=CH), 8.52 (d, 2H; pyrH[3]), 8.43 (m, ArH), 8.04 (t, 1H; pyrH[4]), 7.91–7.20 (m, ArH); ^{13}C NMR ($CDCl_3$): $\delta = 160.30$, 154.83, 148.03, 137.36, 133.99, 128.90, 127.74, 126.82, 126.54, 126.05, 125.99, 123.85, 123.35, 112.92.

2,6-bis[(1-biphenylimino)methyl]pyridine (6): Procedure as for **1**. Off-white solid; yield: 90%. ^{1}H NMR ($CDCl_3$): $\delta = 10.18$ (s, 2H; N=CH), 8.19 (d, 2H; pyrH[3]), 8.09 (t, 1H; pyrH[4]), 7.63–7.17 (m, 18H; ArH); elemental analysis calcd for $C_{31}H_{23}N_3$: C 85.10, H 5.30, N 9.60; found: C 84.52, H 5.21, N 9.48.

2,6-bis[(2,6-diphenylphenylimino)methyl]pyridine (7): Procedure as described for **4**. Yellow solid; yield: 86%. ^{1}H NMR ($CDCl_3$): $\delta = 9.96$ (s, 2H; N=CH), 8.13–6.87 (m, 29H; ArH); ^{13}C NMR ($CDCl_3$): $\delta = 164.8$, 153.9, 139.7, 137.5, 136.8, 133.2, 130.1, 129.8, 129.3, 128.9, 127.9, 127.3, 126.8, 126.6, 125.3, 125.0, 122.8, 122.3, 118.1; mass spectrum (EI): *m/z*: 598 ([M^+], 90), 256 (CH=NAr^+, 100).

Synthesis of complexes

2,6-bis[1-(2-methylphenylimino)ethyl]pyridiliron(II) chloride (8): $FeCl_2$ (0.137 g, 1.08 mmol) was dissolved in hot *n*-butanol (20 mL) at 80 °C. A suspension of 2,6-bis[1-(2-methylphenylimino)ethyl]pyridine (0.37 g; 1.08 mmol) in *n*-butanol was added dropwise at 80 °C. The reaction mixture turned dark blue. After stirring at 80 °C for 15 min, the reaction mixture was allowed to cool to room temperature and stirred overnight. The reaction volume was reduced to a few mL and diethyl ether was added to preciptate the product as a blue powder, which was subsequently washed three times with diethyl ether (10 mL) and dried in vacuo. Dark blue solid; yield: 0.39 g (77%). Mass spectrum: *m/z*: 467 $[M]^+$, 432 $[M-Cl]^+$; elemental analysis calcd for $C_{23}H_{23}N_3FeCl_2 \cdot 0.25\,H_2O$: C 58.44, H 5.01, N 8.89; found: C 58.47, H 5.03, N 8.05; $\mu_{eff} = 5.16\ \mu_B$.

2,6-bis[1-(2,3-dimethylphenylimino)ethyl]pyridiliron(II) chloride (9): Procedure as for **8**. Blue solid; yield: 83%. Mass spectrum: *m/z*: 496 $[M]^+$, 461 $[M-Cl]^+$, 425 $[M-2Cl]^+$; elemental analysis calcd for $C_{25}H_{27}N_3FeCl_2$: C 60.48, H 5.44, N 8.47; found: C 60.01, H 5.02, N 8.10; $\mu_{eff} = 5.53\ \mu_B$. X-ray quality crystals were grown from a saturated acetonitrile solution.

2,6-bis[1-(2,4-dimethylphenylimino)ethyl]pyridiliron(II) chloride (10): Procedure as for **8**. Dark blue solid; yield: 75%. Mass spectrum: *m/z*: 496 $[M]^+$, 461 $[M-Cl]^+$, 425 $[M-2Cl]^+$; elemental analysis calcd for $C_{25}H_{27}N_3FeCl_2$: C 60.48, H 5.44, N 8.47; found: C 59.98, H 5.11, N 8.11; $\mu_{eff} = 5.39\ \mu_B$.

2,6-bis[(2-methylphenylimino)methyl]pyridiliron(II) chloride (11): Procedure as for **8**. Black solid; yield: 93%. Mass spectrum: *m/z*: 404 $[M-Cl]^+$, 369 $[M-2Cl]^+$; elemental analysis calcd for $C_{21}H_{19}N_3FeCl_2$: C 57.31, H 4.35, N 9.54; found: C 57.27, H 4.48, N 9.39; $\mu_{eff} = 5.22\ \mu_B$.

2,6-bis[(1-naphthylimino)methyl]pyridiliron(II) chloride (12): Procedure as for **8**. Brown solid; yield: 71%. Mass spectrum: *m/z*: 511 $[M]^+$, 476 $[M-Cl]^+$, 441 $[M-2Cl]^+$; elemental analysis calcd for $C_{27}H_{19}N_3FeCl_2$: C 63.31, H 3.74, N 8.20; found: C 63.37, H 3.89, N 8.03; $\mu_{eff} = 5.07\ \mu_B$.

2,6-bis[(2-biphenylimino)methyl]pyridiliron(II) chloride (13): Procedure as for **8**. Green-brown solid. Mass spectrum: *m/z*: 563 ([M^+], 40), 528 ([$M-Cl]^+$, 100), 493 ([$M-2Cl]^+$, 28); elemental analysis calcd for $C_{31}H_{23}N_3FeCl_2$: C 65.98, H 4.11, N 7.45; found: C 65.26, H 4.00, N 7.06; $\mu_{eff} = 5.28\ \mu_B$. X-ray quality crystals were grown from a saturated acetonitrile solution.

2,6-bis[(2-biphenylimino)methyl]pyridiliron(II) bromide (14): Procedure as for **8**. Green-brown solid. Elemental analysis calcd for $C_{31}H_{23}N_3FeBr_2$: C 57.00, H 3.55, N 6.43; found: C 56.46, H 3.45, N 6.07. X-ray quality crystals were grown from a saturated acetonitrile solution.

2,6-bis[1-(2-methylphenylimino)ethyl]pyridylcobalt(II) chloride (15): Procedure as for **8**. Green solid; yield: 88%. Mass spectrum: *m/z*: 470 $[M]^+$, 435 $[M-Cl]^+$, 400 $[M-2Cl]^+$; elemental analysis calcd for $C_{23}H_{23}N_3CoCl_2$: C 58.62; H 4.92; N 8.91; found: C 58.33, H 5.25, N 8.40; $\mu_{eff} = 4.65\ \mu_B$.

2,6-bis[(2-methylphenylimino)methyl]pyridylcobalt(II) chloride (16): Procedure as for **8**. Brown solid; yield: 82%. Mass spectrum (FAB): *m/z*: 407 $[M-Cl]^+$, 372 $[M-2Cl]^+$; elemental analysis calcd for $C_{21}H_{19}N_3CoCl_2$: C 56.91, H 4.32, N 9.48; found: C 56.65, H 4.47, N 9.22; $\mu_{eff} = 4.63\ \mu_B$.

2,6-bis[(2,6-diphenylphenylimino)methyl]pyridiliron(II) chloride (17): Procedure as for **8**. Green-brown solid; yield 59%. Mass spectrum (FAB): *m/z*: 716 ([M^+], 5), 680 ([$M-Cl^+$], 40), 256 (CH=NAr^+, 100); elemental analysis calcd for $C_{43}H_{31}N_3FeCl_2$: C 72.08, H 4.36, N 5.86; found: C 72.17, H 4.54, N 5.63. $\mu_{eff} = 4.94\ \mu_B$.

Oligomerisation procedure

a) High-pressure tests: A 1-litre stainless steel reactor was baked out under a nitrogen flow for at least 1 h at >85 °C and subsequently cooled to the temperature of oligomerisation. Isobutane (0.5 L) and MAO (runs 1–11, Table 3) or triisobutylaluminium (runs 12–14, Table 3) were introduced into the reactor and stirred at reaction temperature for at least 1 h. Ethylene was introduced into the reactor by back pressure of nitrogen. The catalyst solution in toluene was then injected under nitrogen. The reactor pressure was maintained constant throughout the oligomerisation run by computer controlled addition of ethylene. The oligomerisation time was 60 min. Runs were terminated by venting off volatiles and the reactor contents was extracted with toluene (400 mL). The toluene solution was washed with dilute hydrochloric acid (1M) and water, dried over $MgSO_4$ and filtered. Quantitative GC analysis of this solution was performed using a weighed aliquot of this solution with a weighed amount of a standard (*n*-heptane).

b) Schlenk-line 1 bar ethylene tests: The precatalyst was dissolved in toluene (40 mL) and MAO (10 wt% in toluene) was added to produce an orange solution. The Schlenk tube was placed in a water bath, purged with ethylene and the contents magnetically stirred and maintained under ethylene (1 bar) for the duration of the oligomerisation. The oligomerisation was terminated by the addition of aqueous hydrogen chloride. Work-up was analogous to that used for the high-pressure tests.

X-ray crystal structure determinations of 9, 13 and 14.

Crystal data for 9: $C_{27}H_{30}N_4Cl_2Fe$, $M_r = 537.3$, monoclinic, $P2_1/n$ (no. 14), $a = 13.461(2)$, $b = 14.948(2)$, $c = 13.779(2)$ Å, $\beta = 106.64(1)^\circ$, $V = 2656.6(7)$ Å^3, $Z = 4$, $\rho_{calcd} = 1.343$ g cm^{-3}, $\mu = 7.91$ cm^{-1}, $F(000) = 1120$, $T = 160$ K; pale blue plates, $0.24 \times 0.10 \times 0.02$ mm, Daresbury SRS Station 9.8 ($\lambda = 0.6878$ Å) with Bruker SMART CCD diffractometer, 0.25° frames with ω scans, 7176 independent reflections. The structure was solved by direct methods and the non-hydrogen atoms were refined anisotropically using full-matrix least-squares based on F^2 to give $R_1 = 0.045$, $wR_2 = 0.110$ for 5356 independent observed absorption corrected reflections [$|F_o| > 4\sigma(|F_o|)$, $2\theta \leq 58^\circ$] and 464 parameters. Restraints were applied to the geometry and anisotropic displacement parameters in the disordered 2,3-dimethylphenyl rings.

Crystal data for 13: $C_{31}H_{23}N_3Cl_2Fe$, $M_r = 564.3$, triclinic, $P\bar{1}$ (no. 2), $a = 9.288(2)$, $b = 12.311(1)$, $c = 14.004(1)$ Å, $\alpha = 108.90(1)$, $\beta = 104.40(1)$, $\gamma = 101.36(1)^\circ$, $V = 1398.3(3)$ Å^3, $Z = 2$, $\rho_{calcd} = 1.340$ g cm^{-3}, $\mu(Cu_{K\alpha}) = 62.7$ cm^{-1}, $F(000) = 580$, $T = 293$ K; deep red platy prisms, $0.27 \times 0.23 \times 0.07$ mm, Siemens P4/PC diffractometer, ω scans, 3719 independent reflections. The structure was solved by direct methods and the non-hydrogen atoms were refined anisotropically using full matrix least-squares based on F^2 to give $R_1 = 0.070$, $wR_2 = 0.176$ for 2645 independent observed absorption corrected reflections [$|F_o| > 4\sigma(|F_o|)$, $2\theta \leq 120^\circ$] and 311 parameters.

Crystal data for 14: $C_{31}H_{23}N_3Br_2Fe$, $M_r = 653.2$, triclinic, $P\bar{1}$ (no. 2), $a = 9.482(1)$, $b = 12.500(1)$, $c = 14.030(1)$ Å, $\alpha = 109.53(1)$, $\beta = 103.74(1)$, $\gamma = 104.12(1)^\circ$, $V = 1424.3(2)$ Å^3, $Z = 2$, $\rho_{calcd} = 1.523$ g cm^{-3}, $\mu(Cu_{K\alpha}) = 77.1$ cm^{-1}, $F(000) = 652$, $T = 293$ K; deep red platy prisms, $0.23 \times 0.20 \times 0.05$ mm, Siemens P4/PC diffractometer, ω scans, 3731 independent reflections. The structure was solved by direct methods and the non-hydrogen atoms were refined anisotropically using full-matrix least-squares based on F^2 to give $R_1 = 0.067$, $wR_2 = 0.160$ for 2511 independent observed absorption corrected reflections [$|F_o| > 4\sigma(|F_o|)$, $2\theta \geq 120^\circ$] and 311 parameters. Crystallographic data (excluding structure factors) for the structures **9, 13** and **14** have been deposited with the Cambridge Crystallographic Data Centre as supplementary publication no. CCDC-139061 (**9**), CCDC-139062 (**13**) and CCDC-139063 (**14**). Copies of the data can be obtained free of charge on application to CCDC, 12 Union Road, Cambridge CB2 1EZ, UK (fax: (+44)1223-336-033; e-mail: deposit@ccdc.cam.ac.uk).

Acknowledgements

BP Amoco Chemicals Ltd. is thanked for financial support and Mr. J. Barton for GC/MS measurements.

[1] D. Vogt in *Applied Homogeneous Catalysis with Organometallic Compounds, Vol. 1* (Eds.: B. Cornils, W. A. Herrmann), VCH, New York, **1996**, pp. 245 – 258.
[2] J. Skupinska, *Chem. Rev.* **1991**, *91*, 613 – 648.
[3] W. Keim, R. P. Schulz, *J. Mol. Catal.* **1994**, *92*, 21 – 33.
[4] W. Keim, *New J. Chem.* **1987**, *11*, 531 – 534.
[5] K. Hirose, W. Keim, *J. Mol. Catal.* **1992**, *73*, 271 – 276.
[6] M. Peuckert, W. Keim, *Organometallics* **1983**, *2*, 594 – 597.
[7] M. Peuckert, W. Keim, *J. Mol. Catal.* **1984**, *22*, 289 – 295.
[8] W. Keim, *Angew. Chem.* **1990**, *102*, 251 – 260; *Angew. Chem. Int. Ed. Engl.* **1990**, *29*, 235 – 244.
[9] W. Keim, *Macromol. Chem. Macromol. Symp.* **1993**, *66*, 225 – 230.
[10] P. Braunstein, Y. Chauvin, S. Mercier, L. Saussine, A. De Cian, J. Fischer, *J. Chem. Soc. Chem. Commun.* **1994**, 2203 – 2204.
[11] D. Matt, M. Huhn, J. Fischer, A. De Cian, W. Kläui, I. Tkatchenko, M. C. Bonnet, *J. Chem. Soc. Dalton Trans.* **1993**, 1173 – 1178.
[12] K. A. Ostoja Starzewski, J. Witte, *Angew. Chem.* **1987**, *99*, 76 – 77; *Angew. Chem. Int. Ed.* **1987**, *26*, 63 – 74.
[13] K. A. Ostoja Starzewski, J. Witte in *Transition Metal Catalyzed Polymerizations - Ziegler Natta and Metathesis Polymerization* (Ed.: R. P. Quirk), Cambridge University Press, Cambridge, **1988**, pp. 472 – 496.
[14] K. A. Ostoja Starzewski, J. Witte, K. H. Reichert, G. Vasiliou in *Transition Metals and Organometallics as Catalysts for Olefin Polymerization* (Eds.: W. Kaminsky, H. Sinn), Springer, Berlin, **1988**, pp. 349 – 360.
[15] W. Keim, F. H. Kowalt, R. Goddard, C. Krüger, *Angew. Chem.* **1978**, *90*, 493 – 494; *Angew. Chem. Int. Ed. Engl.* **1978**, *17*, 466 – 467.
[16] K. Keim, A. Behr, B. Limbäcker, C. Krüger, *Angew. Chem.* **1983**, *95*, 505; *Angew. Chem. Int. Ed. Engl.* **1983**, *22*, 503.
[17] S. Y. Desjardins, K. J. Cavell, H. Jin, B. W. Skelton, A. H. White, *J. Organomet. Chem.* **1996**, *515*, 233 – 243.
[18] A. Behr, V. Falbe, U. Freudenberg, W. Keim, *Isr. J. Chem.* **1986**, *27*, 277 – 279.
[19] K. J. Cavell, *Aust. J. Chem.* **1994**, *47*, 769 – 797.
[20] G. A. Foulds, A. M. A. Bennet, M. L. Niven, D. A. Thornton, K. J. Cavell, S. Desjardins, E. J. Peacock, *J. Mol. Catal.* **1994**, *87*, 117 – 136.
[21] K. J. Cavell, A. F. Masters, *J. Chem. Research (S)* **1983**, 72 – 73.
[22] K. J. Cavell, A. F. Masters, *Aust. J. Chem.* **1986**, *39*, 1129 – 1134.
[23] R. Abeywickrema, M. A. Bennett, K. J. Cavell, M. Kony, A. F. Masters, A. G. Webb, *J. Chem. Soc. Dalton Trans.* **1993**, 59 – 68.
[24] M. C. Bonnet, F. Dahan, A. Ecke, W. Keim, R. P. Schulz, I. Tkatchenko, *J. Chem. Soc. Chem. Commun.* **1994**, 615.
[25] G. J. P. Britovsek, W. Keim, S. Mecking, D. Sainz, T. Wagner, *J. Chem. Soc. Chem. Commun.* **1993**, 1632 – 1634.
[26] S. A. Svejda, M. Brookhart, *Organometallics* **1999**, *18*, 65 – 74.
[27] C. M. Killian, L. K. Johnson, M. Brookhart, *Organometallics* **1997**, *16*, 2005 – 2007.
[28] S. Strömberg, M. Oksman, L. Zhang, K. Zetterberg, *Acta Chem. Scand.* **1995**, *49*, 689 – 695.
[29] P.-L. Bres, V. C. Gibson, C. D. F. Mabille, W. Reed, D. F. Wass, R. H. Weatherhead (BP Chemicals Ltd.), WO 98/49208, **1998** [*Chem. Abstr.* **1999**, *130*, 4185].
[30] S. Plentz Meneghetti, P. J. Lutz, J. Kress, *Organometallics* **1999**, *18*, 2734 – 2737.
[31] T. V. Laine, K. Lappalainen, J. Liimatta, E. Aitola, B. Löfgren, M. Leskelä, *Macromol. Rapid Commun.* **1999**, *20*, 487 – 491.
[32] T. V. Laine, M. Klinga, A. Maaninen, E. Aitola, M. Leskelä, *Acta Chem. Scand.* **1999**, *53*, 968 – 973.
[33] A. Köppl, H. G. Alt (Phillips Petroleum Company), US 5,932,670, **1999** [*Chem. Abstr.* **1999**, *131*, 116669].
[34] S. Y. Desjardins, A. A. Way, M. C. Murray, D. Adirim, M. C. Baird, *Organometallics* **1998**, *17*, 2382 – 2384.
[35] E. K. van den Beuken, W. J. J. Smeets, A. L. Spek, B. L. Feringa, *Chem. Commun.* **1998**, 223 – 224.
[36] T. Alderson, E. L. Jenner, J. Lindsey, R. V., *J. Am. Chem. Soc.* **1965**, *87*, 5638 – 5645.
[37] A. D. Ketley, L. P. Fisher, A. J. Berlin, C. R. Morgan, E. H. Gorman, T. R. Steadman, *Inorg. Chem.* **1967**, *6*, 657 – 663.
[38] N. H. Phung, G. Lefebvre, *C. R. Acad. Sci. (Paris) Ser. C* **1967**, *265*, 519 – 521.
[39] G. Hata, *Chem. Ind.* **1965**, 223.
[40] L. Sun Pu, A. Yamamoto, S. Ikeda, *J. Am. Chem. Soc.* **1968**, *90*, 7170 – 7171.
[41] F. Bouachir, B. Chaudret, I. Tkatchenko, *J. Chem. Soc. Chem. Commun.* **1986**, 94 – 95.
[42] F. Bouachir, B. Chaudret, F. Dahan, F. Agbossou, I. Tkatchenko, *Organometallics* **1991**, *10*, 455 – 462.
[43] K. Kawakami, T. Mizoroki, A. Ozaki, *Bull. Chem. Soc. Jpn.* **1978**, *51*, 21 – 24.
[44] R. Cramer, *J. Am. Chem. Soc.* **1965**, *87*, 4717 – 4727.
[45] G. Braca, G. Sbrana, *Chim. Ind.* **1974**, *56*, 110 – 116.
[46] B. L. Small, M. Brookhart, *J. Am. Chem. Soc.* **1998**, *120*, 7143 – 7144.
[47] G. J. P. Britovsek, V. C. Gibson, B. S. Kimberley, P. J. Maddox, S. J. McTavish, G. A. Solan, A. J. P. White, D. J. Williams, *Chem. Commun.* **1998**, 849 – 850.
[48] B. L. Small, M. Brookhart, *Polym. Prep. (Am. Chem. Soc. Div. Polym. Chem.)* **1998**, *39*, 213.
[49] B. L. Small, M. Brookhart, A. M. A. Bennett, *J. Am. Chem. Soc.* **1998**, *120*, 4049 – 4050.
[50] A. M. A. Bennett (DuPont), WO 98/27124, **1998** [*Chem. Abstr.* **1998**, *129*, 122973x].

  0947-6539/00/0612-2230 $ 17.50+.50/0

[51] G. J. P. Britovsek, B. A. Dorer, V. C. Gibson, B. S. Kimberley, G. A. Solan (BP Chemicals Ltd.), WO 99/12981, **1999** [*Chem. Abstr.* **1999**, *130*, 252793].
[52] G. J. P. Britovsek, M. Bruce, V. C. Gibson, B. S. Kimberley, P. J. Maddox, S. Mastroianni, S. J. McTavish, C. Redshaw, G. A. Solan, S. Strömberg, A. J. P. White, D. J. Williams, *J. Am. Chem. Soc.* **1999**, *121*, 8728–8740.
[53] B. L. Small, M. Brookhart, *Macromolecules* **1999**, *32*, 2120–2130.
[54] M. S. Brookhart, B. L. Small (DuPont/UNC), WO 98/30612, **1998** [*Chem. Abstr.* **1998**, *129*, 149375r].
[55] C. Pellecchia, M. Mazzeo, D. Pappalardo, *Macromol. Rapid Commun.* **1998**, *19*, 651–655.
[56] M. S. Brookhart, B. L. Small (DuPont/UNC), WO 99/02472, **1999** [*Chem. Abstr.* **1999**, *130*, 139754].
[57] It proved possible to obtain paramagnetic contact-shifted spectra for the more soluble di-substituted derivatives (see ref. [52]).
[58] J. D. Scollard, D. H. McConville, N. C. Payne, J. J. Vittal, *Macromolecules* **1996**, *29*, 5241–5243.
[59] J. D. Scollard, D. H. McConville, *J. Am. Chem. Soc.* **1996**, *118*, 10008–10009.
[60] J. D. Scollard, D. H. McConville, S. J. Rettig, *Organometallics* **1997**, *16*, 1810–1812.
[61] J. D. Scollard, D. H. McConville, J. J. Vittal, *Organometallics* **1997**, *16*, 4415–4420.
[62] J. D. Scollard, D. H. McConville, J. J. Vittal, N. C. Payne, *J. Mol. Catal.* **1998**, *128*, 201–214.
[63] V. C. Gibson, B. S. Kimberley, A. J. P. White, D. J. Williams, P. Howard, *Chem. Commun.* **1998**, 313–314.
[64] F. Jäger, H. W. Roesky, H. Dorn, S. Shah, M. Noltemeyer, H.-G. Schmidt, *Chem. Ber./Recueil* **1997**, *130*, 399–403.
[65] F. Guérin, D. H. McConville, N. C. Payne, *Organometallics* **1996**, *15*, 5085–5089.
[66] F. Guérin, D. H. McConville, J. J. Vittal, *Organometallics* **1996**, *15*, 5586–5590.
[67] M. Aizenberg, L. Turculet, W. M. Davis, F. Schattenmann, R. R. Schrock, *Organometallics* **1998**, *17*, 4795–4812.
[68] M. A. Flores, M. R. Manzoni, R. Baumann, W. M. Davis, R. R. Schrock, *Organometallics* **1999**, *18*, 3220–3227.
[69] L.-C. Liang, R. R. Schrock, W. M. Davis, D. H. McConville, *J. Am. Chem. Soc.* **1999**, *121*, 5797–5798.
[70] P. H. M. Budzelaar, A. B. van Oort, A. G. Orpen, *Eur. J. Inorg. Chem.* **1998**, 1485–1494.
[71] V. C. Gibson, P. J. Maddox, C. Newton, C. Redshaw, G. A. Solan, A. J. P. White, D. J. Williams, *Chem. Commun.* **1998**, 1651–1652.
[72] L. K. Johnson, C. M. Killian, M. Brookhart, *J. Am. Chem. Soc.* **1995**, *117*, 6414–6415.
[73] C. M. Killian, D. J. Tempel, L. K. Johnson, M. Brookhart, *J. Am. Chem. Soc.* **1996**, *118*, 11664.
[74] S. J. McLain, J. Feldman, E. F. McCord, K. H. Gardner, M. F. Teasley, E. B. Coughlin, K. J. Sweetman, L. K. Johnson, M. Brookhart, *Macromolecules* **1998**, *31*, 6705–6707.
[75] C. Pellecchia, A. Zambelli, M. Mazzeo, D. Pappalardo, *J. Mol. Catal.* **1998**, *128*, 229–237.
[76] T. Schleis, J. Heinemann, T. P. Spaniol, R. Mülhaupt, J. Okuda, *Inorg. Chem. Commun.* **1998**, *1*, 431–434.
[77] C. Wang, S. Friedrich, T. R. Younkin, R. T. Li, R. H. Grubbs, D. A. Bansleben, M. W. Day, *Organometallics* **1998**, *17*, 3149–3151.
[78] T. Schleis, T. P. Spaniol, J. Okuda, J. Heinemann, R. Mülhaupt, *J. Organomet. Chem.* **1998**, *569*, 159–167.
[79] F. Guérin, O. Del Vecchio, D. H. McConville, *Polyhedron* **1998**, *17*, 917–923.
[80] M. Atiqullah, H. Hammawa, H. Hamid, *Eur. Polym. J.* **1998**, *34*, 1511–1520.
[81] P. G. T. Fogg, W. Gerrard, *Solubility of gases in liquids*, Wiley, West Sussex, England, **1991**.
[82] V. Busico, R. Cipullo, *Macromolecules* **1994**, *27*, 7538–7543.
[83] U. Stehling, J. Diebold, R. Kirsten, W. Röll, H.-H. Brintzinger, S. Jüngling, R. Mülhaupt, F. Langhauser, *Organometallics* **1994**, *13*, 964–970.
[84] T. Tsutsui, A. Mizuno, N. Kashiwa, *Polymer* **1989**, *30*, 428–431.
[85] H. H. Brintzinger, D. Fischer, R. Mülhaupt, B. Rieger, R. M. Waymouth, *Angew. Chem.* **1995**, *107*, 1255–1283; *Angew. Chem. Int. Ed.* **1995**, *34*, 1143–1170.
[86] L. Deng, Woo, T. K., Cavallo, L., Margl, P. M., Ziegler, T., *J. Am. Chem. Soc.* **1997**, *119*, 6177–6186.
[87] A. R. Siedle, W. M. Lamanna, R. A. Newmark, J. N. Schroepfer, *J. Mol. Catal.* **1998**, *128*, 257–271.
[88] A. R. Siedle, W. M. Lamanna, R. A. Newmark, J. Stevens, D. E. Richardson, M. Ryan, *Macromol. Chem., Macromol. Symp.* **1993**, *66*, 215–224.
[89] A. R. Siedle, W. M. Lamanna, J. M. Olofson, B. A. Nerad, R. A. Newmark, *ACS Symp. Ser.* **1993**, *517*, 156–167.
[90] M. E. Thompson, S. M. Baxter, A. R. Bulls, B. J. Burger, M. C. Nolan, B. D. Santarsiero, W. P. Schaeffer, J. E. Bercaw, *J. Am. Chem. Soc.* **1987**, *109*, 203–219.
[91] B. J. Burger, M. E. Thompson, W. D. Cotter, J. E. Bercaw, *J. Am. Chem. Soc.* **1990**, *112*, 1566–1577.
[92] T. Ziegler, E. Folga, A. Berces, *J. Am. Chem. Soc.* **1993**, *115*, 636–646.
[93] P. J. Shapiro, W. D. Cotter, W. P. Schaefer, J. A. Labinger, J. E. Bercaw, *J. Am. Chem. Soc.* **1994**, *116*, 4623–4640.
[94] T. K. Woo, P. M. Margl, T. Ziegler, P. E. Blöchl, *Organometallics* **1997**, *16*, 3454–3468.
[95] N. W. Alcock, R. G. Kingston, P. Moore, C. Pierpoint, *J. Chem. Soc. Dalton Trans.* **1984**, 1937–1943.
[96] Y. Miura, H. Oka, M. Momoki, *Synthesis* **1995**, 1419–1422.

Received: November 25, 1999 [F2156]